

Article

Nano-Surface Composite Coating Reinforced by Ta₂C, Al₂O₃ and MWCNTs Nanoparticles for Aluminum Base via FSP

Essam B. Moustafa ^{1,*}, Waheed Sami Abushanab ², Ammar Melaibari ^{1,3}, Anastasia V. Mikhaylovskaya ⁴, Mohamed Shaaban Abdel-Wahab ³ and Ahmed O. Mosleh ^{4,5}

¹ Mechanical Engineering Department, Faculty of Engineering, King Abdulaziz University, Jeddah 80204, Saudi Arabia; aamelaibari@kau.edu.sa

² Marine Engineering Department, Faculty of Maritime Studies and Marine Engineering, King Abdulaziz University, Jeddah 21589, Saudi Arabia; wabushanab@kau.edu.sa

³ Center of Nanotechnology, King Abdulaziz University, Jeddah 21589, Saudi Arabia; msahassan@kau.edu.sa

⁴ Department of Physical Metallurgy of Non-Ferrous Metals, National University of Science and Technology "MISIS", Leninsky Prospekt, 4, 119049 Moscow, Russia; mikhaylovskaya@isis.ru (A.V.M.); mosleh@isis.ru (A.O.M.)

⁵ Mechanical Engineering Department, Shoubra Faculty of Engineering, Benha University, Cairo 11629, Egypt

* Correspondence: abmostafa@kau.edu.sa

Abstract: In the present work, an advanced technique was applied to coat an Al 2024 alloy with a surface composite layer reinforced with various nanoparticles. The surface of Al 2024 aluminum alloy was modified with Ta₂C, Al₂O₃ and multi wall carbon nanotubes MWCNTs nanoparticles by friction stir process (FSP). An improvement in the surface of the fabricated nanocomposite due to the refinement of the microstructure grains was achieved. In addition, a significant improvement in the hardness and wear behavior was observed. The reinforcement particles were incorporated into double and triple hybrid composite particles to determine the most effective combination for the controlled properties. The results showed that for the composite reinforced with a double hybrid of Al₂O₃ and MWCNTs, the microstructure grains of the fabricated nanocomposite surface were refined by 40 times. The hardness was significantly improved, i.e., it was increased by 48% by incorporating the triple reinforcement (Ta₂C, Al₂O₃, and MWCNTs) into the surface of Al 2024 aluminum alloy. The results of wear properties were in agreement with the results of hardness; the maximum wear resistance was obtained for Al 2024-Ta₂C + Al₂O₃ + MWCNTs, and the wear rate was reduced by 11 times.

Keywords: metal matrix composites (MMCs); wear resistance; ceramics; nanoconfinement; grain refinement; friction stir processing



Citation: Moustafa, E.B.; Abushanab, W.S.; Melaibari, A.; Mikhaylovskaya, A.V.; Abdel-Wahab, M.S.; Mosleh, A.O. Nano-Surface Composite Coating Reinforced by Ta₂C, Al₂O₃ and MWCNTs Nanoparticles for Aluminum Base via FSP. *Coatings* **2021**, *11*, 1496. <https://doi.org/10.3390/coatings11121496>

Received: 1 November 2021

Accepted: 3 December 2021

Published: 5 December 2021

Publisher's Note: MDPI stays neutral with regard to jurisdictional claims in published maps and institutional affiliations.



Copyright: © 2021 by the authors. Licensee MDPI, Basel, Switzerland. This article is an open access article distributed under the terms and conditions of the Creative Commons Attribution (CC BY) license (<https://creativecommons.org/licenses/by/4.0/>).

1. Introduction

The incorporation of one or more different reinforcing particles into metals greatly improves the fabricated metal matrix composite [1,2]. A light metal matrix alloy such as aluminum matrix composites AMMCs has attracted much attention in contemporary engineering [3,4]. Due to its light weight and unique mechanical properties, aluminum alloy is the ideal choice for the fabrication of metal composites using various techniques [5,6]. The fabrication of metal matrix hybrid composites has become more accessible in recent years due to the revolution in fabrication and processing techniques such as FSP, laser melting, etc. [7,8]. The FSP process is considered one of the most effective methods for fabricating metal matrix composite surfaces because of its ability to introduce various reinforcing nanoparticles into the metal base without significant obstacles during the fabrication process [9,10]. The FSP method has been used to improve and modify the surface properties of processed aluminum alloys by using reinforced particles and ceramic materials such as Al₂O₃, B₄C, SiC, VC, CWNTs, TiB₂ and others [11–18]. The hybrid

composites exhibit excellent strength properties, uniformity and significantly improved microstructural behavior. SiC and Al₂O₃ nanoparticles have been used to improve the wear resistance and microhardness of an aluminum alloy [19]. Moreover, the refinement of microstructure significantly affects the mechanical properties due to equiaxed grains produced by FSP process or by the addition of chemical modifiers [20–22].

One of the most difficult goals of researchers is to improve the wear resistance of aluminum alloys and their composites. Several authors have addressed this problem in the literature, for example [10,23–31]. The reinforcement particles have been incorporated into mono and hybrid composites to improve the surface of the aluminum matrix. The hard ceramic particles such as SiC and other similar particles significantly affect the hardness, but on the contrary, the wear resistance has not improved noticeably [32]. By using hybrid reinforcement particles such as Cr and SiC, the wear performance of the Al-Si alloy was improved by using the standard casting process. Due to their exceptional hardness, the SiC/Cr particles significantly limit the scratching of the composite surface [33]. The hardness behavior of the hybrid composite of CNTs/Al₂O₃-Al 365 was improved by the infiltration technique; thus, it reached 110 of 52 HV, the compressive strengths of the hybrid MMCs increased with increasing Al₂O₃ content [34]. Therefore, the previous works in the literature investigated the mechanical properties, microstructure and wear behavior of the hybrid composite matrices using similar reinforcement particles. In the current work, we focus on using different types of reinforcement particles with different properties and morphologies of particle shapes to investigate their effects on the mechanical properties, microstructure and wear behavior. Moreover, the FSP approach has been used to fabricate a novel hybrid metal composite matrix consisting of three different families of reinforcement particles (Ta₂C + Al₂O₃ + MWCNTs)/Al 2024.

2. Materials and Methods

Al 2024 aluminum sheets were used to prepare nanocomposites with aluminum metal matrix surfaces. The chemical composition of the Al 2024 alloy sheets in the as-prepared state is shown in Table 1. The surface of the base alloy was reinforced with MWCNTs and Al₂O₃ nanoparticles and Ta₂C particles supplied by Nanoshel-UK-Ltd (Congleton, UK). The densities of the particles used are listed in Table 2. The process was carried out using the Friction Stir Processing (FSP) technique via an automatic milling machine (Bridgeport, Elmira, NY, USA) to produce the nanocomposite surface on the Al 2024 alloy sheets. The typical fabrication process of the nanocomposite surface using the friction stir process (FSP) is illustrated in Figure 1a.

Table 1. Chemical composition of the as-received Al 2024 aluminum wt.%.

Cu	Mg	Mn	Si	Fe	Al
4.1	1.6	0.3	0.1	0.1	Balance

Table 2. The densities of the Al 2024 aluminum alloy and the reinforcement particles.

Element	Density, g/cm ³
Al 2024	2.78
Ta ₂ C	14.30
Al ₂ O ₃	3.90
MWCNTs	2.10

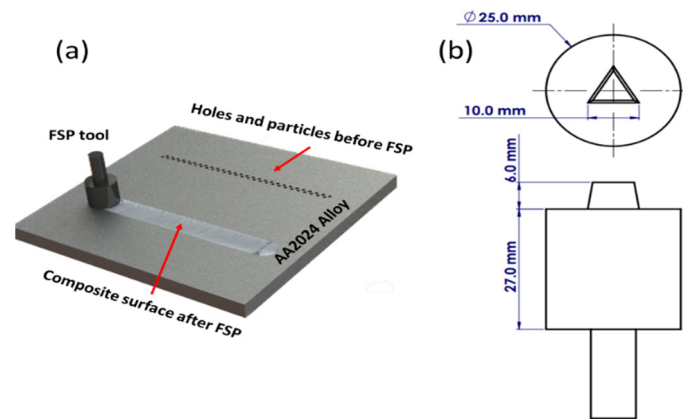


Figure 1. (a) Typical fabrication process of the nanocomposite surface using the friction stir process (FSP), and (b) design of the FSP tool.

The rotational speed of the FSP tool was 1100 rpm, the linear traverse speed was 30 mm/min, and the tilt angle was 1° , which were chosen according to [35]. Figure 1a shows the fabrication of the nanocomposite surface using the FSP. A triangular conical pin was used to stir the mixture; the design and dimensions of the tool are shown in Figure 1b. The plates were drilled to a depth of 5 mm and a diameter of 2 mm. Two methods were used to introduce the reinforcing nanoparticles into the grooved holes: In the first method, two mixed reinforcing particles (dual hybrid composites) such as $\text{Ta}_2\text{C} + \text{Al}_2\text{O}_3$, $\text{Ta}_2\text{C} + \text{MWCNTs}$, $\text{Al}_2\text{O}_3 + \text{MWCNTs}$ were used. In the second case, the three additives were combined to prepare a triple hybrid composite of $\text{Ta}_2\text{C} + \text{Al}_2\text{O}_3 + \text{MWCNTs}$ (Table 3). In addition, the hybrid particles were mixed before being added to the primary matrix.

Table 3. The combination of the reinforcement particles into the Al 2024 aluminum alloy matrix.

Al 2024-H1	$\text{Ta}_2\text{C} + \text{Al}_2\text{O}_3$	Al 2024-H3	$\text{Al}_2\text{O}_3 + \text{MWCNTs}$
Al 2024-H2	$\text{Ta}_2\text{C} + \text{MWCNTs}$	Al 2024-H4	$\text{Ta}_2\text{C} + \text{Al}_2\text{O}_3 + \text{MWCNTs}$

The Al_2O_3 , MWCNTs and Ta_2C particles were examined by transmission electron microscopy (TEM, JSM -200F, JEOL, Tokyo, Japan). For TEM characterization, a Branson type ultrasonic bath (CPX5800H-E, Emerson, St. Louis, MO, USA) was used to thoroughly disperse the particles in a combination of ethyl alcohol and deionized water. The sample was then loaded onto copper-coated carbon grids of size 200 mesh. The TEM analyzes show the different morphologies of the nanomaterials. Thin cylinders characterize MWCNTs. Voluminous spheres characterize Ta_2C particles. The average particle size of Al_2O_3 and Ta_2C was 17.3 ± 2 nm and 280 ± 4.5 nm, respectively, while the size of MWCNTs was 40 ± 3 nm inner diameter and 80 ± 6 nm outer diameter. Scanning electron microscopy (SEM; XL30, Philips, Amsterdam, The Netherlands) and optical microscopy (Olympus BX51, Miami, FL, USA) were used to investigate the microstructure of the generated surface nanostructures. The samples for microstructure analysis were mechanically ground and polished and then etched; the preparation procedures were described in detail in [36]. In addition, the Rockwell hardness testing machine (True Blue United Testing Systems, Devens, MA, USA) was used to determine the Vickers microhardness according to the ASTM E-384-17 specification [15]. To establish the hardness profile, the Vickers microhardness readings had to be measured on the entire specimen surface in all machining areas. The wear test was performed for 10 min at 256 rpm with a load of 0.3 bar on a 316 stainless steel cylinder (200 mm diameter) in accordance with ASTM G99-04A [37] at room temperature. Prior to each test, the cylinder was cleaned with acetone to remove surface contaminants; hence the wear specimens used in this method acted as a pin. At ordinary room temperature, the friction coefficient was measured by pin-on-disk tribometers (CSM Instruments, Peseux, Switzerland).

3. Results and Discussion

Increasing the mechanical properties and improving the wear resistance of Al 2024 aluminum alloy should not be accompanied by an increase in weight, which is considered one of the benefits of this alloy. Thus, it is essential to calculate the increase in the density of the manufactured composites.

The manufactured composite's volume can be calculated as in Equations (1) and (2):

$$\text{volume of composite } (V_C) = \text{Volume of particles } (V_p) + \text{Volume of matrix } (V_m) \quad (1)$$

$$V_C = \text{projected area of tool} \times \text{length of the processed composite} \quad (2)$$

Equations (3) and (4) can be used to calculate the volume of the nano-reinforcements and the base matrix:

$$V_p = \text{of holes along the processed composite} \times \text{volume of each hole} \quad (3)$$

$$V_m = V_C - V_p \quad (4)$$

Thus, Equations (5) and (6) can be used to determine the volume fraction of the nano-reinforcements and the base matrix:

$$\text{Volume fraction of particles } (VF_p) = \frac{V_p}{V_C} \quad (5)$$

$$\text{Volume fraction of matrix } VF_m = \frac{V_m}{V_C} \quad (6)$$

After determining the volume of nano-reinforced particles and the base matrix, the theoretical density of the produced composite can be calculated using the following equations (Equations (7) and (8)):

$$\text{Density of composite } (\rho_c) = \frac{\text{Mass of composite } (M_c)}{\text{Volume of composite } (V_c)} = \frac{M_p + M_m}{V_c} \quad (7)$$

$$\rho_c = \frac{(\rho_p \times V_p) + (\rho_m V_m)}{V_c} \quad (8)$$

The theoretical densities of the fabricated surface nanocomposites reinforced with hybrid and tripod nanoparticles are summarized in Table 4. The reinforcement nanoparticles accounted for 11.7% of the volume of the fabricated nanocomposites. In general, the reinforcement of the Al 2024 aluminum alloy matrix with hybrid or triple components increased the densities of the fabricated surface nanocomposites (Table 4, last column). The increase in densities with respect to the base matrix alloy is shown in Figure 2. Due to its high density, Ta₂C has a significant effect on increasing the density of the fabricated surface nanocomposites containing Ta₂C. The maximum increase in density, 27%, was obtained when H1, Ta₂C and Al₂O₃ were incorporated, while the minimum increase in density, 1%, was recorded when H3, Al₂O₃ and MWCNTs were used as reinforcement materials.

Table 4. Fabricated surface nanocomposites' density.

Composite	ρ_{pr} g/cm ³	V_{pr} cm ³	ρ_M g/cm ³	V_m cm ³	V_c cm ³	ρ_c g/cm ³
Al 2024-H1	9.1	0.44	2.78	3.33	3.77	3.52
Al 2024-H2	8.2	0.44	2.78	3.33	3.77	3.41
Al 2024-H3	3.0	0.44	2.78	3.33	3.77	2.81
Al 2024-H4	6.8	0.44	2.78	3.33	3.77	3.25

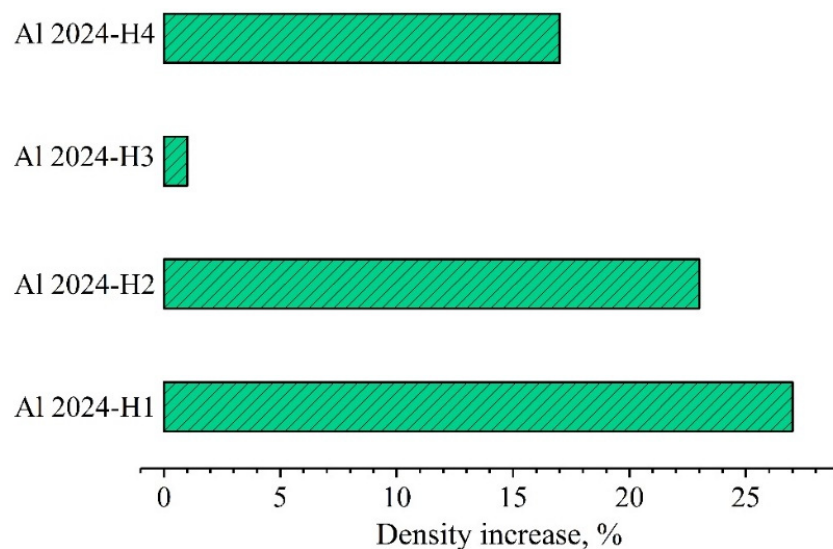


Figure 2. Density increases (%), with respect to base matrix alloy, Al 2024 aluminum alloy.

4. Microstructure Analysis

The TEM image of the reinforcing particles is shown in Figure 3. Al_2O_3 and MWCNTs appear in nano size, while Ta_2C can be seen in microparticle size. Figure 4 shows the microstructure of Al 2024 aluminum alloy sheets in the initial state and after friction stir processing without reinforcement. The microstructure of the as-prepared samples shows elongated, non-recrystallized grains due to the cold rolling process (Figure 4a). It can be observed that the intermetallic phases [1] formed in the aluminum matrix were coarse and unevenly distributed in the as-rolled specimens after the rolling process (Figure 4a). The microstructure was significantly changed after the friction stirring process. Specific microstructure regions were formed after the friction stirring process: the heat-affected zone (HAZ), the thermomechanical heat-affected zone (TMAZ), and the stirred or nugget zone (SZ), as shown in Figure 4b. Extreme plastic deformation generated additional heat in the stirred zone during the friction stirring process, resulting in a dynamically recrystallized (DRX) grain (Figure 4 area 2). This hypothesis explains why the stirred zone consists of uniformly equiaxed grains rather than the base metal (BM). Due to the plastic deformation and heat flux generated (Figure 4 area 1). The material was subjected to thermal cycling in the heat-affected zone without plastic deformation, resulting in the only insignificantly altered microstructure.

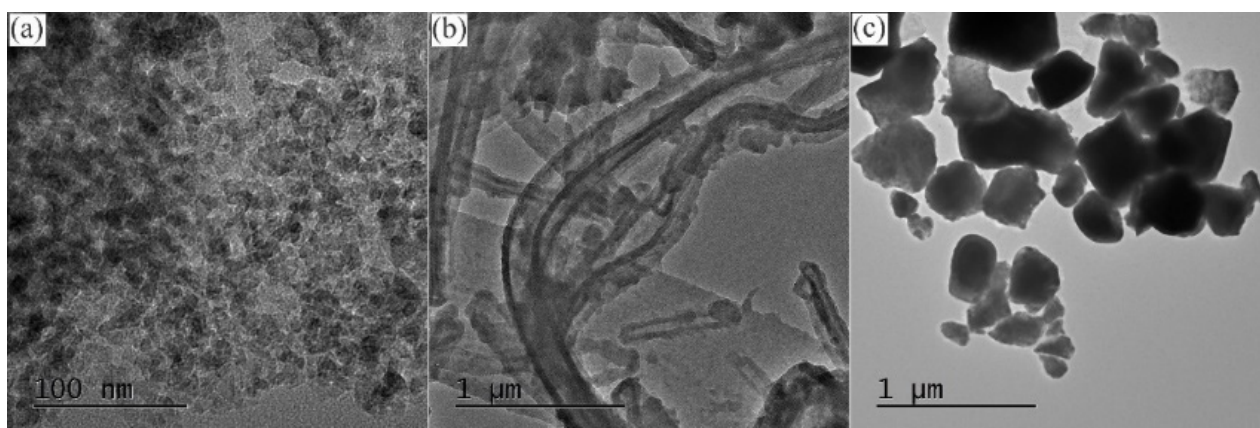


Figure 3. TEM image of the reinforcement particles. (a) Al_2O_3 nanoparticles, (b) MWCNTs, and (c) Ta_2C particles.

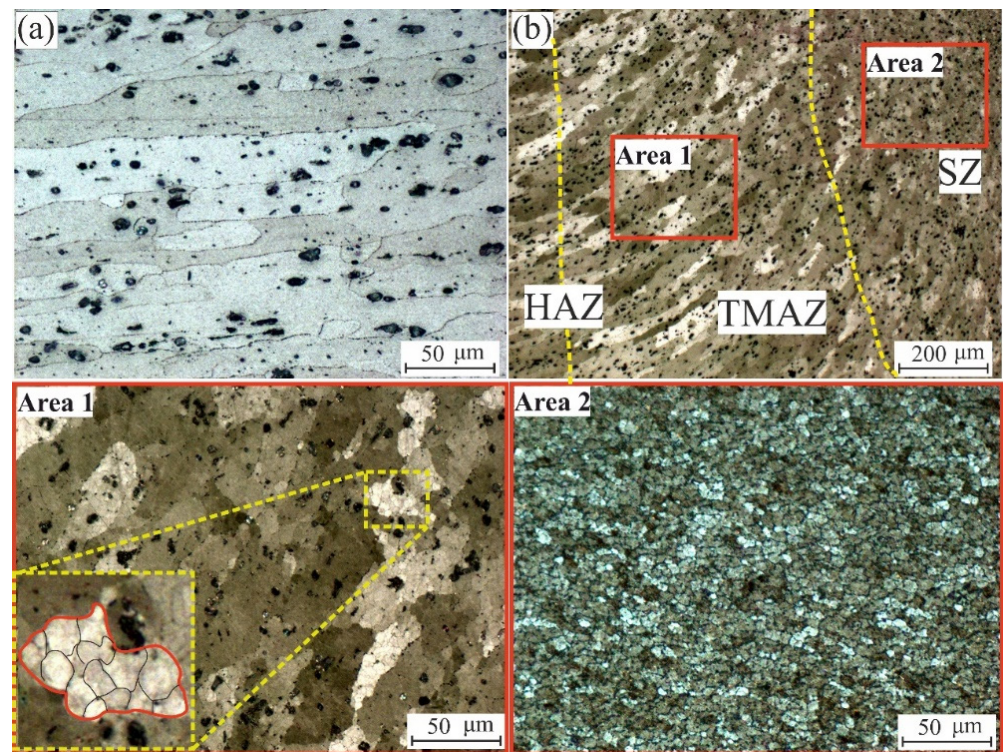


Figure 4. The typical microstructure image (a) as-received Al 2024 alloy sheets and (b) the friction stir processed zones.

Figure 5 shows the microstructure of the fabricated surface nanocomposites for nano-reinforcements, H1 (Figure 5a), H2 (Figure 5b), H3 (Figure 5c), and H4 (Figure 5d). In general, the incorporation of nano-reinforcements into the studied metal matrix, Al 2024, resulted in significant grain refinement in the stirred zone. It is known that the presence of nano-reinforcement particles in the metal matrix during the stirring friction process increases the nucleation centers, resulting in many new grains. Moreover, the nano-reinforcements prevent grain growth in the stirred zone after the dynamic recrystallization process (DRX) [38]. The average grain size and corresponding aspect ratio of the starting material after FSP and the fabricated surface nanocomposites are listed in Table 5. It can be observed that the average grain size decreased greatly after FSP. Moreover, the grains are almost equiaxed with an aspect ratio of about ≈ 1 . The reinforcing particles have led to further refinement in addition to the pure FSP effect. Figure 6 shows the grain size refinement of the FSP treated and the fabricated composites with respect to the Al 2024 alloy aluminum sheet in the as-prepared condition. After the FSP process, the grains were refined by 22 times of the initial Al 2024 alloy aluminum sheet. The grain refinement in the produced composites varies between 33 and 40 times, depending on the type of reinforcement particles.

Table 5. The average grain size of the as-received alloy, after FSP, and manufactured surface nanocomposites.

–	Al 2024-BM	Al 2024-FSP	Al 2024-H1	Al 2024-H2	Al 2024-H3	Al 2024-H4
Average Grain size, μm	180 ± 40	7.5 ± 1.5	4.8 ± 1.1	5.4 ± 1.1	4.4 ± 0.9	4.6 ± 0.8
Aspect ratio (length/width)	5.5	1.02	1.1	1.05	1.02	1.02

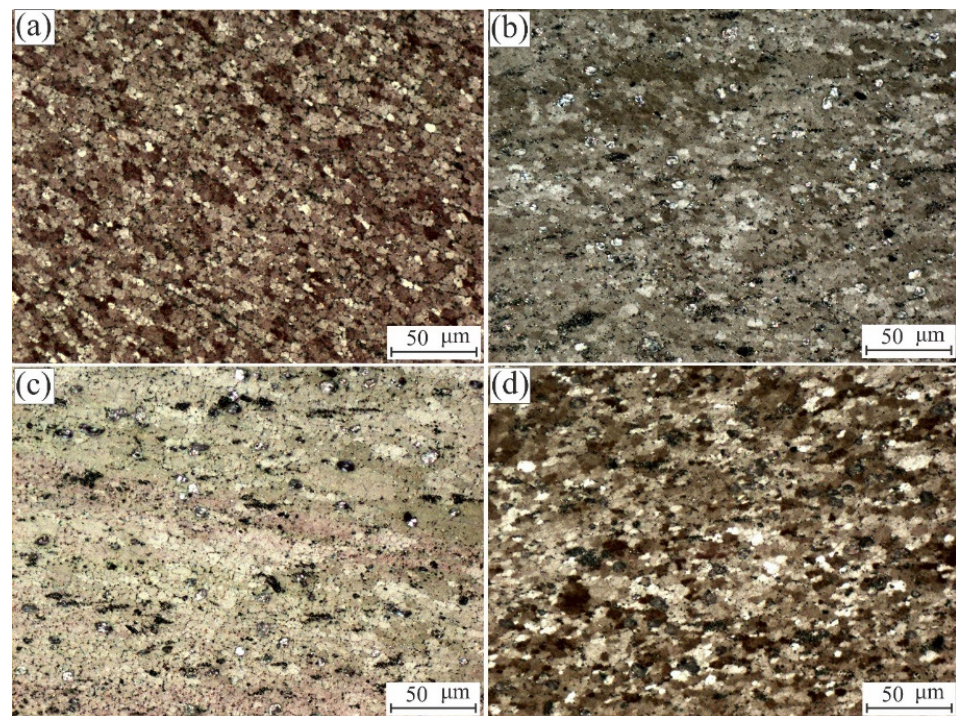


Figure 5. The microstructure of the stirred zone of the manufactured surface nanocomposites: (a) Al 2024-H1, (b) Al 2024-H2, (c) Al 2024-H3, and (d) Al 2024-H4.

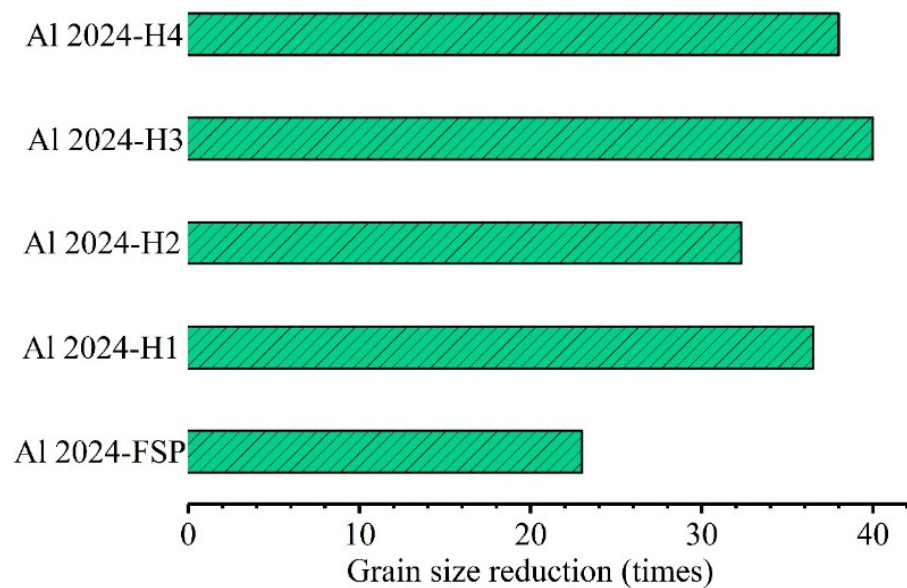


Figure 6. Grain size refinement with respect to base alloy, Al 2024 aluminum alloy.

Figure 7 shows the SEM and Energy Dispersive X-Ray Spectroscopy EDS mapping images of the fabricated hybrid triple particle reinforced surface nanocomposite, Al 2024-H4. In this study, the EDS mapping showed the distribution of the reinforcement particles, the accumulation of the unwanted clusters of the reinforced nanoparticles. It is found that the Ta₂C particles are uniformly distributed in the matrix. The results of SEM and EDS verified the incorporation of the reinforcements into the fabricated surface nanocomposite. After FSP, the distribution of Al₂O₃ nanoparticles and MWCNTs in the Al 2024-H4 composite was uniform; no aggregation or accumulation of these particles was observed. A small amount of Ta₂C was found to be aggregated in the fabricated surface nanocomposite, which was due to the large size of these particles. In general, most of the Ta₂C was uniformly

distributed in the matrix. The uniform distribution of the reinforcement particles in the SZ positively affected the properties of the fabricated composites, such as the hardness and wear behavior. The more uniform the distribution of reinforcement particles is, the more uniform and regular the properties are throughout the SZ. Therefore, the uniform distribution of reinforcement particles is a key issue and challenge in the fabrication of composites, which has been achieved here.

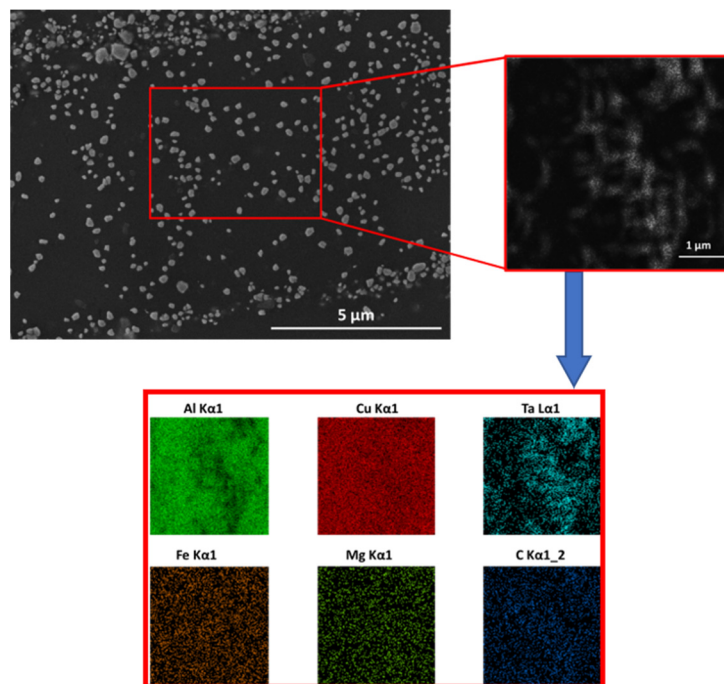


Figure 7. SEM and EDS mapping images of triple additive hybrid composite.

5. Hardness Characterization

Figure 8 illustrates the Vickers microhardness profiles and the improvements in the hardness of the Al 2024 aluminum alloy sheet. The average hardness of the as-prepared Al 2024 aluminum alloy sheets was 97 ± 5 HV. After FSP, the hardness values in SZ decreased due to the softening effect in SZ (Figure 8a) [37,39,40]. The decrease in hardness values was about 20% compared to BM (Figure 8b). The addition of reinforcing nanoparticles improved the hardness in the SZ, and the improvement in hardness was significantly dependent on the type of reinforcing nanoparticles. In general, the surface nanocomposites reinforced with Ta₂C, Al 2024-H1, H2, and H4 exhibited high hardness in the SZ (Figure 8a), while the Al 2024-H3 composite showed less improvement. The maximum improvement in hardness was observed for Al 2024-H4; it was 48% higher than Al 2024 base alloy (Figure 8a). Reinforcement of a hybrid of Al₂O₃ and Ta₂C resulted in a hardness improvement of 36% over the Al 2024 alloy. It can be observed that the thermomechanical and heat-affected zones are the weakest areas since no nanoparticles were reinforced in these areas. Moreover, the elongated grains, which were partially restored, resulted in lower hardness in these areas (Figure 8a). Another important observation was the slight fluctuation in hardness in the SZ of all the composites prepared, which confirmed the uniform distribution of the reinforced nanoparticles in the SZ.

Figure 9 shows the experimental wear rate due to weight loss and the improvements in wear rate with respect to the base alloy. The wear rate of Al 2024 aluminum alloy plates was 0.065 mg/s. After FSP, the wear rate decreased to 0.0183 mg/s, which was due to the refinement in SZ and the uniform distribution of the intermetallic in SZ compared to BM (Figure 9a). The introduction of reinforcing nanoparticles into the Al 2024 matrix resulted in a significant decrease in the wear rate of the fabricated composites. The type of reinforcing nanoparticles played a major role in improving the wear resistance of the

fabricated composites. The wear rate was compatible with the hardness results. The surface nanocomposites reinforced with Ta₂C, Al 2024-H2, H1 and H4 exhibited a lower wear rate in SZ (Figure 9a). The lowest wear rate was observed for Al 2024-H4; the wear resistance was 11 times higher than BM (Figure 9b). The highest wear rate, 0.00733 mg/s, was obtained by adding H3.

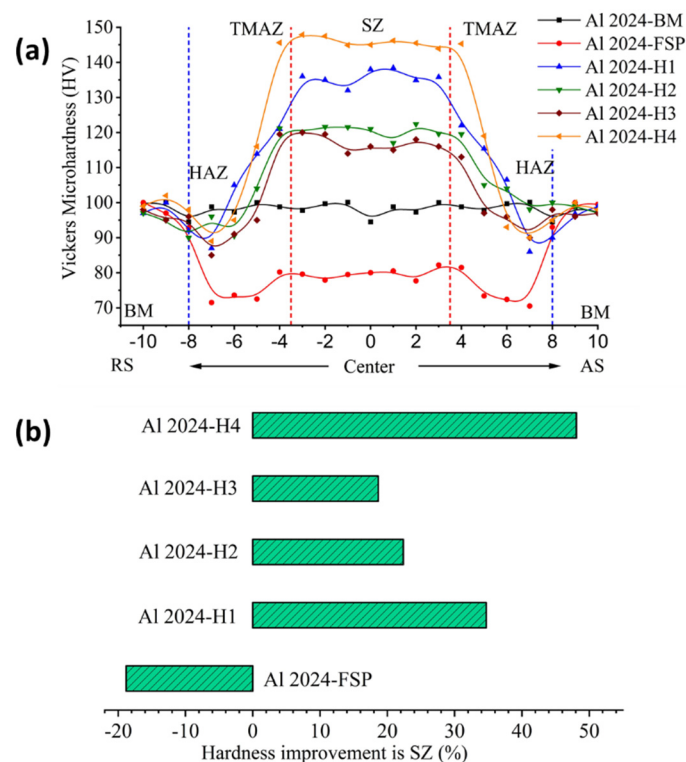


Figure 8. (a) Vickers micro-hardness profile of the matrix, after FSP, and manufactured surface nanocomposite, and (b) the hardness improvement in the SZ of the manufactured nanocomposites.

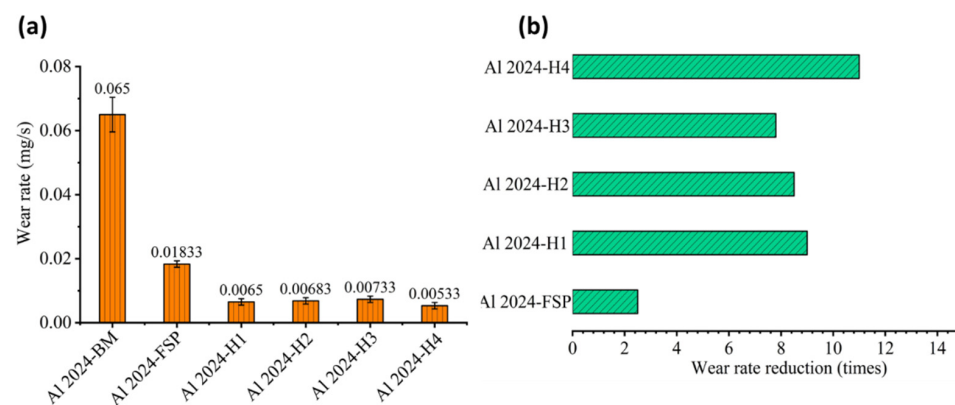


Figure 9. (a) wear rate, (b) wear rate reduction concerning the base alloy.

Figure 10 shows the profile of the coefficient of friction as a function of sliding time. The coefficient of friction shows a slightly increasing trend. After the transition period, the rough trend of the curve becomes stable, indicating that the wear rate has changed from the initial wear in the transition state to the steady-state wear rate. In addition, the surface roughness parameters play an important role in evaluating the friction coefficient; therefore, the initial transition wear rate lasts longer than that of the composites with lower roughness. The presence of MWCNTs particles in the hybrid composite matrix decreases the value of the friction coefficient. Figure 11 shows the average value of the coefficient of friction. Accordingly, the hybrid composite Al 2024-H3 exhibits the lowest coefficient

of friction among the specimens investigated. The coefficient of friction increased due to the additional grain refinement that occurred in the stirred zone, as seen in the FSPed sample, which has the highest value due to the extra plastic deformation that occurred in the absence of the reinforcing particles. These results were confirmed by the curve of the hardness profile described in the previous section.

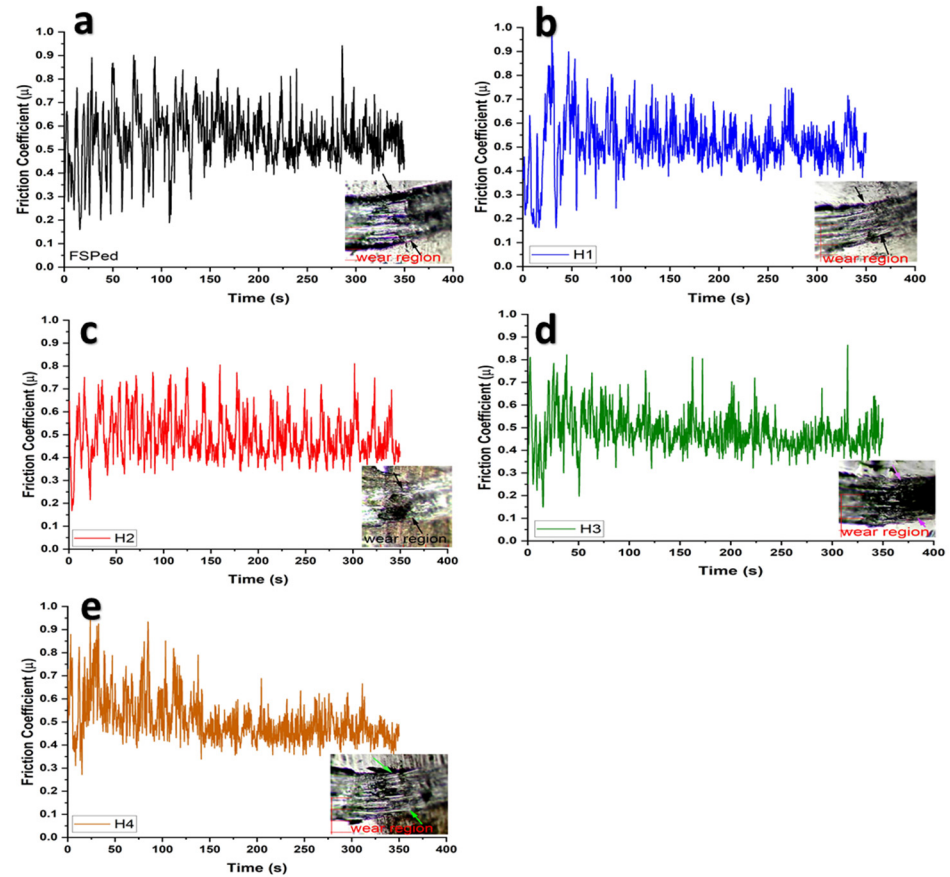


Figure 10. Friction coefficient profile, (a) the friction stir processed wear zone, (b) Al 2024-H1, (c) Al 2024-H2, (d) Al 2024-H3, and (e) Al 2024-H4.

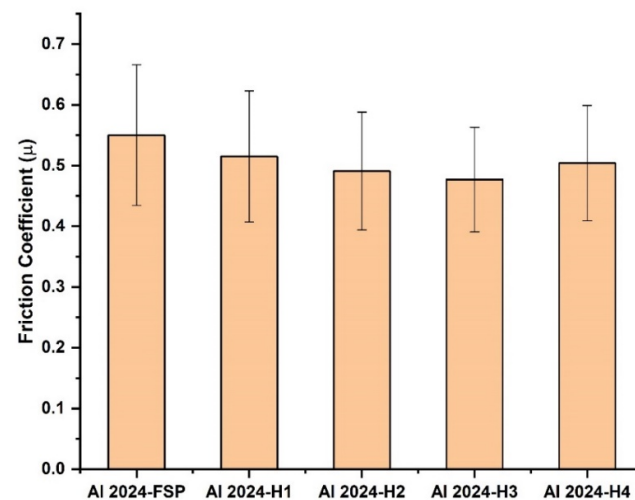


Figure 11. Mean value of the friction coefficient.

6. Conclusions

Different dual and triple reinforcing nanoparticles strengthened the aluminum alloy sheets Al 2024 by friction stirring method. In this study, Ta₂C + Al₂O₃, Ta₂C + MWCNTs, Al₂O₃ + MWCNTs and Ta₂C + Al₂O₃ + MWCNTs were used as reinforcement combinations. The physical (density), mechanical, and wear behavior of the fabricated composites were characterized. After analyzing the data, we can conclude that:

- The incorporation of the different dual and triple reinforcement increased the density of the fabricated composites. The Ta₂C particles were the most important reinforcement in increasing the density as they have extremely high density compared to the other reinforcement materials. The maximum increase in density, 27%, was observed for Al 2024/Ta₂C + Al₂O₃, while the minimum, 1%, was observed for Al 2024/Al₂O₃ + MWCNTs.
- The incorporation of reinforcement nanoparticles into the studied metal matrix resulted in additional grain refinement in the stirred zone compared to the FSP samples. The average grain size in the SZ of the fabricated composites was 33-40 times smaller than that of the as-prepared aluminum alloy sheet Al 2024. The maximum taper was observed for Al 2024-H3 (Al₂O₃ + MWCNTs); this can be attributed to the size of the reinforcement nanoparticles. The SEM and EDS also confirmed the uniform distribution of all particles in the matrix.
- The reinforcement of Al 2024 alloy with these particles significantly increased the hardness in the SZ. The presence of the triple reinforcement, Al₂O₃ + MWCNTs + Ta₂C, resulted in a maximum hardness enhancement of 48%. The minimum hardness enhancement, 20%, was observed for the dual hybrid Al₂O₃ + MWCNTs particles.
- The wear results were compatible with the hardness results. The incorporation of reinforcing nanoparticles in the studied metal matrix increased the wear resistance of this alloy. The maximum improvement in wear, 11 times of BM, was obtained by the addition of triple reinforcement, Al₂O₃ + MWCNTs + Ta₂C. The minimum increase in wear resistance was found to be eight times that of the base metal alloy, which was achieved by double reinforcement of Al₂O₃ and MWCNTs nanoparticles.

Author Contributions: Data curation, A.V.M.; formal analysis, W.S.A.; investigation, E.B.M.; methodology, A.O.M. and M.S.A.-W.; supervision, A.M. All authors have read and agreed to the published version of the manuscript.

Funding: This project was funded by the deanship of scientific research (DSR) at King Abdulaziz University, Jeddah (Grant No. RG-3-150-38). The authors therefore gratefully acknowledge technical and financial support from DSR.

Institutional Review Board Statement: Not applicable.

Informed Consent Statement: Not applicable.

Data Availability Statement: Data sharing is not applicable to this article.

Acknowledgments: This research was funded by the Deanship of Scientific Research (DSR), King Abdulaziz University, Jeddah, under Grant No. RG-3-150-38. Therefore, the authors gratefully acknowledge technical and financial support from the ministry of education and King Abdulaziz University, DSR, Jeddah, Saudi Arabia.

Conflicts of Interest: The authors declare no conflict of interest.

References

1. Essam, B.; Moustafa, A.M.K.; Haitham, M.; Ahmed, M.H.; Mosleh, A.O. Microstructure, hardness, and wear behavior investigation of the surface nanocomposite metal matrix reinforced by silicon carbide and alumina nanoparticles. *J. Miner. Metal Mater. Eng.* **2021**, *7*, 57–62. [[CrossRef](#)]
2. Abushanab, W.S.; Moustafa, E.B.; Melaibari, A.A.; Kotov, A.D.; Mosleh, A.O. A novel comparative study based on the economic feasibility of the ceramic nanoparticles role's in improving the properties of the AA5250 nanocomposites. *Coatings* **2021**, *11*, 977. [[CrossRef](#)]

3. Essam, B.; Moustafa, S.M.; Abdel-Wanis, S.; Mahmoud, T.; El-Kady, E.-S. Review multi pass friction stir processing. *Am. Sci. Res. J. Eng. Technol. Sci. (ASRJETS)* **2016**, *22*, 98–108.
4. Jalilvand, M.M.; Mazaheri, Y. Effect of mono and hybrid ceramic reinforcement particles on the tribological behavior of the AZ31 matrix surface composites developed by friction stir processing. *Ceram. Int.* **2020**, *46*, 20345–20356. [[CrossRef](#)]
5. Moustafa, E.B. Dynamic Characteristics study for surface composite of amncs matrix fabricated by friction stir process. *Materials* **2018**, *11*, 1240. [[CrossRef](#)]
6. Khalil, A.M.; Loginova, I.; Pozdniakov, A.V.; Mosleh, A.O.; Solonin, A.N. Evaluation of the microstructure and mechanical properties of a new modified cast and laser-Melted AA7075 alloy. *Materials* **2019**, *12*, 3430. [[CrossRef](#)]
7. Maamoun, A.H.; Veldhuis, S.C.; Elbestawi, M. Friction stir processing of AlSi10Mg parts produced by selective laser melting. *J. Mater. Process. Technol.* **2018**, *263*, 308–320. [[CrossRef](#)]
8. Aziz, S.S.A.; Abulkhair, H.; Moustafa, E.B. Role of hybrid nanoparticles on thermal, electrical conductivity, microstructure, and hardness behavior of nanocomposite matrix. *J. Mater. Res. Technol.* **2021**, *13*, 1275–1284. [[CrossRef](#)]
9. Li, K.; Liu, X.; Zhao, Y. Research Status and Prospect of Friction Stir Processing Technology. *Coatings* **2019**, *9*, 129. [[CrossRef](#)]
10. Moustafa, E.B. Effect of multi-pass friction stir processing on mechanical properties for AA2024/Al₂O₃ nanocomposites. *Materials* **2017**, *10*, 1053. [[CrossRef](#)]
11. Baradeswaran, A.; Perumal, A.E. Study on mechanical and wear properties of Al 7075/Al₂O₃/graphite hybrid composites. *Compos. Part. B Eng.* **2014**, *56*, 464–471. [[CrossRef](#)]
12. Eskandari, H.; Taheri, R. A novel technique for development of aluminum alloy matrix/TiB₂/Al₂O₃ hybrid surface nanocomposite by friction stir processing. *Procedia Mater. Sci.* **2015**, *11*, 503–508. [[CrossRef](#)]
13. Karpasand, F.; Abbasi, A.; Ardestani, M. Effect of amount of TiB₂ and B₄C particles on tribological behavior of Al7075/B₄C/TiB₂ mono and hybrid surface composites produced by friction stir processing. *Surf. Coat. Technol.* **2020**, *390*, 125680. [[CrossRef](#)]
14. Mazahery, A.; Shabani, M.O. Investigation on mechanical properties of nano-Al₂O₃-reinforced aluminum matrix composites. *J. Compos. Mater.* **2011**, *45*, 2579–2586. [[CrossRef](#)]
15. Moustafa, E.B.; Melaibari, A.; Basha, M. Wear and microhardness behaviors of AA7075/SiC-BN hybrid nanocomposite surfaces fabricated by friction stir processing. *Ceram. Int.* **2020**, *46*, 16938–16943. [[CrossRef](#)]
16. Moustafa, E.B.; Taha, M.A. Preparation of high strength graphene reinforced Cu-based nanocomposites via mechanical alloying method: Microstructural, mechanical and electrical properties. *Appl. Phys. A* **2020**, *126*, 220. [[CrossRef](#)]
17. Ostovan, F.; Amanollah, S.; Toozandehjani, M.; Shafiei, E. Fabrication of Al5083 surface hybrid nanocomposite reinforced by CNTs and Al₂O₃ nanoparticles using friction stir processing. *J. Compos. Mater.* **2019**, *54*, 1107–1117. [[CrossRef](#)]
18. Rana, H.G.; Badheka, V.J.; Kumar, A. Fabrication of Al7075 / B₄C surface composite by novel friction stir processing (FSP) and investigation on wear properties. *Procedia Technol.* **2016**, *23*, 519–528. [[CrossRef](#)]
19. James, J.; Venkatesan, K.; Kuppan, P.; Ramanujam, R. Comparative study of composites reinforced with SiC and TiB₂. *Procedia Eng.* **2014**, *97*, 1012–1017. [[CrossRef](#)]
20. Umanath, K.; Selvamani, S.T.; Palanikumar, K.; Sabarikreeshwaran, R. Dry sliding wear behaviour of AA6061-T6 reinforced SiC and Al₂O₃ particulate hybrid composites. *Procedia Eng.* **2014**, *97*, 694–702. [[CrossRef](#)]
21. AbuShanab, W.S.; Moustafa, E.B. Effects of friction stir processing parameters on the wear resistance and mechanical properties of fabricated metal matrix nanocomposites (MMNCs) surface. *J. Mater. Res. Technol.* **2020**, *9*, 7460–7471. [[CrossRef](#)]
22. Dieguez, T.; Burgueño, A.; Svoboda, H. Superplasticity of a friction stir processed 7075-T651 aluminum alloy. *Procedia Mater. Sci.* **2012**, *1*, 110–117. [[CrossRef](#)]
23. Essam, B.; Moustafa, S.M.; Abdel-Wanis, S.; Mahmoud, T. Surface composite defects of Al/Al₂O₃ metal matrix fabricated by Friction stir processing. *J. Mater. Sci. Surf. Eng.* **2017**, *5*, 524–527. [[CrossRef](#)]
24. Akbari, M.; Shojaefard, M.H.; Asadi, P.; Khalkhali, A. Wear and mechanical properties of surface hybrid metal matrix composites on Al-Si aluminum alloys fabricated by friction stir processing. *Proc. Inst. Mech. Eng. Part. L J. Mater. Des. Appl.* **2017**, *233*, 790–799. [[CrossRef](#)]
25. Aruri, D.; Adepu, K.; Adepu, K.; Bazavada, K. Wear and mechanical properties of 6061-T6 aluminum alloy surface hybrid composites [(SiC+Gr) and (SiC+Al₂O₃)] fabricated by friction stir processing. *J. Mater. Res. Technol.* **2013**, *2*, 362–369. [[CrossRef](#)]
26. Ezazi, M.A.; Quazi, M.M.; Zalnezhad, E.; Sarhan, A.A.D. Enhancing the tribo-mechanical properties of aerospace AL7075-T6 by magnetron-sputtered Ti/TiN, Cr/CrN & TiCr/TiCrN thin film ceramic coatings. *Ceram. Int.* **2014**, *40*, 15603–15615. [[CrossRef](#)]
27. Jayavelu, S.; Mariappan, R.; Rajkumar, C. Wear characteristics of sintered AA2014 with alumina and titanium di-Boride metal matrix composites. *Int. J. Ambient. Energy* **2018**, *42*, 173–178. [[CrossRef](#)]
28. Kurt, H.I.; Oduncuoğlu, M.; Asmatulu, R. Wear behavior of aluminum matrix hybrid composites fabricated through friction stir welding process. *J. Iron Steel Res. Int.* **2016**, *23*, 1119–1126. [[CrossRef](#)]
29. Mahmoud, E.R.; Takahashi, M.; Shibayanagi, T.; Ikeuchi, K. Wear characteristics of surface-hybrid-MMCs layer fabricated on aluminum plate by friction stir processing. *Wear* **2010**, *268*, 1111–1121. [[CrossRef](#)]
30. Mehta, K.M.; Badheka, V.J. Wear behavior of boron-carbide reinforced aluminum surface composites fabricated by Friction Stir Processing. *Wear* **2019**, *426–427*, 975–980. [[CrossRef](#)]
31. Paidar, M.; Ojo, O.O.; Ezatpour, H.R.; Heidarzadeh, A. Influence of multi-pass FSP on the microstructure, mechanical properties and tribological characterization of Al/B₄C composite fabricated by accumulative roll bonding (ARB). *Surf. Coat. Technol.* **2019**, *361*, 159–169. [[CrossRef](#)]

32. Yuvaraj, N.; Aravindan, S. Vipin wear characteristics of Al5083 surface hybrid nano-composites by friction stir processing. *Trans. Indian Inst. Met.* **2016**, *70*, 1111–1129. [[CrossRef](#)]
33. Zayed, A.S.; Kamel, B.M.; Osman, T.A.; Elkady, O.A.; Ali, S. Experimental study of tribological and mechanical properties of aluminum matrix reinforced by Al₂O₃/CNTs. *Fuller. Nanotub. Carbon Nanostruct.* **2019**, *27*, 538–544. [[CrossRef](#)]
34. Daniel, A.A.; Murugesan, S.; Manojkumar; Sukkasamy, S. Dry Sliding Wear Behaviour of Aluminium 5059/SiC/MoS₂ Hybrid Metal Matrix Composites. *Mater. Res.* **2017**, *20*, 1697–1706. [[CrossRef](#)]
35. Kumar, J.; Singh, D.; Kalsi, N.S.; Sharma, S.; Pruncu, C.I.; Pimenov, D.Y.; Rao, K.V.; Kapłonek, W. Comparative study on the mechanical, tribological, morphological and structural properties of vortex casting processed, Al–SiC–Cr hybrid metal matrix composites for high strength wear-resistant applications: Fabrication and characterizations. *J. Mater. Res. Technol.* **2020**, *9*, 13607–13615. [[CrossRef](#)]
36. Kim, H.H.; Babu, J.S.S.; Kang, C.G. Fabrication of A356 aluminum alloy matrix composite with CNTs/Al₂O₃ hybrid reinforcements. *Mater. Sci. Eng. A* **2013**, *573*, 92–99. [[CrossRef](#)]
37. Moustafa, E.B.; Abushanab, W.S.; Melaibari, A.; Yakovtseva, O.; Mosleh, A.O. The effectiveness of incorporating hybrid reinforcement nanoparticles in the enhancement of the tribological behavior of aluminum metal matrix composites. *JOM* **2021**, 1–11. [[CrossRef](#)]
38. Moustafa, E.B. Hybridization effect of BN and Al₂O₃ nanoparticles on the physical, wear, and electrical properties of aluminum AA1060 nanocomposites. *Appl. Phys. A* **2021**, *127*, 724. [[CrossRef](#)]
39. Barlow, I.C.; Jones, H.; Rainforth, W.M. Evolution of microstructure and hardening, and the role of Al₃Ti coarsening, during extended thermal treatment in mechanically alloyed Al–Ti–O based materials. *Acta Mater.* **2001**, *49*, 1209–1224. [[CrossRef](#)]
40. Moustafa, E.B.; Melaibari, A.; Alsuruji, G.; Khalil, A.M.; Mosleh, A.O. Tribological and mechanical characteristics of AA5083 alloy reinforced by hybridising heavy ceramic particles Ta₂C & VC with light GNP and Al₂O₃ nanoparticles. *Ceram. Int.* **2021**. [[CrossRef](#)]